SLAS Discovery
2019, Vol. 24(7) 745–754


DOI: 10.1177/2472555219853220
journals.sagepub.com/home/jbx
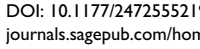

Evaluation of Luminogenic Substrates as Probe Substrates for Bacterial Cytochrome P450 Enzymes: Application to *Mycobacterium tuberculosis*

Sandra Ortega Ugalde[1], Dongping Ma[2], James J. Cali[2], and Jan N. M. Commandeur[1]

Abstract

Several cytochrome P450 enzymes (CYPs) encoded in the genome of *Mycobacterium tuberculosis* (Mtb) are considered potential new drug targets due to the essential roles they play in bacterial viability and in the establishment of chronic intracellular infection. Identification of inhibitors of Mtb CYPs at present is conducted by ultraviolet-visible (UV-vis) optical titration experiments or by metabolism studies using endogenous substrates, such as cholesterol and lanosterol. The first technique requires high enzyme concentrations and volumes, while analysis of steroid hydroxylation is dependent on low-throughput analytical methods. Luciferin-based luminogenic substrates have proven to be very sensitive substrates for the high-throughput profiling of inhibitors of human CYPs. In the present study, 17 pro-luciferins were evaluated as substrates for Mtb CYP121A1, CYP124A1, CYP125A1, CYP130A1, and CYP142A1. Luciferin-BE was identified as an excellent probe substrate for CYP130A1, resulting in a high luminescence yield after addition of luciferase and adenosine triphosphate (ATP). Its applicability for high-throughput screening was supported by a high Z'-factor and high signal-to-background ratio. Using this substrate, the inhibitory properties of a selection of known inhibitors could be characterized using significantly less protein concentration when compared to UV-vis optical titration experiments. Although several luminogenic substrates were also identified for CYP121A1, CYP124A1, CYP125A1, and CYP142A1, their relatively low yield of luminescence and low signal-to-background ratios make them less suitable for high-throughput screening since high enzyme concentrations will be needed. Further structural optimization of luminogenic substrates will be necessary to obtain more sensitive probe substrates for these Mtb CYPs.

Keywords

cytochrome P450, *Mycobacterium tuberculosis*, tuberculosis, bioluminescence, high-throughput screening

Introduction

Cytochrome P450 enzymes (CYPs or P450s) constitute a superfamily of heme thiolate containing proteins that catalyze the oxidation of a wide range of physiological and non-physiological compounds. The enzymes are represented in virtually all kingdoms of life.[1–3] In bacteria, most identified CYPs still remain orphan enzymes with unknown function. Functional characterization of several bacterial CYPs has revealed that they can catalyze widely diverse reactions, such as the degradation of organic compounds as a source of carbon for microbial growth or the synthesis of bioactive metabolites.[4] CYPs from pathogenic bacteria have become attractive therapeutic drug targets. For example, CYP51 is a validated drug target, since 14α-demethylation of sterol substrates is required for the biosynthesis of membrane sterols, such as cholesterol in animals and ergosterol in fungi.[5] CYP51 is strongly inhibited by various azole

[1]AIMMS-Division of Molecular Toxicology, Faculty of Science, Vrije Universiteit, Amsterdam, North-Holland, The Netherlands
[2]Promega Corporation, Madison, WI, USA

Received Dec 16, 2018, and in revised form Apr 28, 2019. Accepted for publication May 2, 2019.

Supplemental material is available online with this article.

Corresponding Author:
Jan N. M. Commandeur, Division of Molecular Toxicology, Amsterdam Institute for Molecules Medicines and Systems (AIMMS), Faculty of Sciences, Vrije Universiteit, De Boelelaan 1108, 1081 HZ Amsterdam, The Netherlands.
Email: j.n.m.commandeur@vu.nl

antibiotics, such as clotrimazole, econazole, fluconazole, and ketoconazole, which are capable of binding tightly to the active site of CYP51 by direct coordination of the imidazole and triazole group to the heme iron.[6,7] The inhibition of CYP51 has therefore been proposed as a treatment for infectious diseases, such as Chagas and the African sleeping sickness disease, which are caused by protozoan parasites containing a CYP51 orthologue.[8,9]

Genome mapping of *Mycobacterium tuberculosis* (Mtb), the etiologic agent of tuberculosis (TB), has revealed that it encodes a *CYP51* gene (*Rv0764c*) as well as an additional 19 *CYP* genes.[10] Some of these CYPs appear to play pivotal roles in Mtb viability and the establishment of chronic infection, and may represent potential novel drug targets for this disease. Several azole compounds bind with high affinity to several Mtb CYPs, and some were shown to have a potent antimycobacterial activity against (non-)persistent Mtb in mice as well as against multidrug-resistant TB strains (MDR-TB).[11–21] These azole-containing drugs, however, also strongly inhibit human CYPs, which could lead to adverse drug reactions due to drug–drug interactions. Therefore, the search for potent and more specific inhibitors for Mtb CYPs is still actively pursued.

To date, screening for potential inhibitors of Mtb CYPs is most commonly conducted by using UV-vis optical titration experiments in which the affinity of ligands is determined by spectroscopically recording the concentration-dependent shift of the heme iron Soret band.[17,22,23] Enzyme inhibition experiments are only feasible for the Mtb CYPs for which substrates have been identified. Analysis of metabolites of identified substrates of Mtb CYPs, such as cholesterol,[20] methyl branched lipids,[24] dicyclotyrosine (cYY),[15,16] and dextromethorphan,[25] depends on gas or liquid chromatography coupled to mass spectrometry. These methods are relatively low-throughput and time-consuming, especially when extractions and derivatization reactions are required, as in the case of gas chromatography.[24] Therefore, there is still a need for suitable probe substrates that will enable high-throughput screening (HTS) of libraries of potential inhibitors of Mtb CYPs.

Bioluminescent assays based on the light production by the adenosine triphosphate (ATP)-dependent metabolism of D-luciferin by luciferase are widely used for many applications because of their high sensitivity and the possibility to apply them in high-density microplates.[26] So-called pro-luciferins have been developed as substrates of human CYPs and are used for HTS of inhibition or induction of human CYPs.[27–29] These assays are based on O-dealkylation or aromatic hydroxylation reactions catalyzed by human CYPs, resulting in formation of D-luciferin or 2-cyano-6-hydroxybenzothiazole that can be converted to D-luciferin by reaction with D-cysteine.[27–29] Because of the very high sensitivity of D-luciferin detection by ATP–luciferase reagent by luminometers, these assays require only low amounts of CYPs and can be performed in high-density microplates. The aim of the present study was to evaluate 17 D-luciferin-based luminogenic analogues as potential probe substrates for CYP121A1, CYP124A1, CYP125A1, CYP130A1, and CYP142A1 from Mtb.

Materials and Methods

Materials

Genomic DNA from Mtb strain H37Rv was provided by Prof. Dr. Wilbert Bitter (Medical Microbiology and Infection Control, Vrije Universiteit [VU] Medical Center, Amsterdam, the Netherlands) and was used as template DNA for the cloning of Mtb CYPs. *Escherichia coli* DNA was isolated from DH5α cells using the High-Pure PCR Template Preparation Kit (Roche Molecular Systems, Woerden, the Netherlands). Primers (**Table 1**) were from Integrated DNA Technologies BVBA (Leuven, Belgium). D-Luciferin, P450-Glo Luciferin Detection Reagent (P450-Glo LDR), and pro-luminogenic substrates were from Promega (Madison, WI, USA). The following pro-luminogenic substrates were used (for structures, see **Suppl. Fig. S1**): Luciferin-BE, Luciferin-CEE, Luciferin-H EGE, Luciferin-H, Luciferin-IPA, Luciferin-ME, Luciferin-ME EGE, Luciferin-Multi-CYP, Luciferin-PFBE, Luciferin-PPXE, Luciferin-1A2, Luciferin-2B6, Luciferin-2J2 /4F12, Luciferin-3A7, Luciferin-4A, Luciferin-4F2/3, and Luciferin-4F1. NADPH (Nicotinamide adenine dinucleotide phosphate in reduced form) was from AppliChem GmbH (Darmstadt, Germany). Glucose-6-phosphate, glucose-6-phosphate dehydrogenase from *Leuconostoc mesenteroides*, porcine esterase, D-cysteine, econazole, and miconazole were obtained from Sigma-Aldrich (Schnelldorf, Germany). Ketoconazole was purchased from Fagron (Rotterdam, the Netherlands). All other chemicals and reagents were of analytical grade and obtained from standard suppliers unless otherwise mentioned.

Molecular Cloning, Expression, and Purification of Selected Mtb CYPs and Surrogate Redox Partners

The PCR amplifications of the genes coding for CYP121A1 (*Rv2276*), CYP124A1 (*Rv2266*), CYP125A1 (*Rv3534c*), and CYP142A1 (*Rv1256c*) and the surrogate redox partners from *E. coli* DH5α, ferredoxin NADPH reductase (FNR), and flavodoxin (Flda) were conducted using the upstream and downstream primers shown in **Table 1**. The corresponding recombinant enzymes were expressed in *E. coli* BL21 (DE3) and purified as described elsewhere.[30] CYP130A1 and CYP130A1-BM3R, the fusion protein of CYP130A1 with the reductase domain of CYP102A1, were expressed and purified as described previously.[25]

Table 1. Oligonucleotide primers used in plasmid construction.

Direction	Primer Sequence	Restriction Site
F-CYP121A1	5′-**CATATG**ACCGCGACCGTTCTG-3′	NdeI
R-CYP121A1	5′-**AAGCTT**ATCCTACCAGAGCACCGG-3′	HindIII
F-CYP124A1	5′-**CATATG**GGGCCTCAACACGGC-3′	NdeI
R-CYP124A1	5′-**AAGCTT**TCAGGACCACGTAACTGG-3′	HindIII
F-CYP125A1	5′-**CATATG**GTGTCGTGGAATCACCAGT-3′	NdeI
R-CYP125A1	5′-**TCTAGAT**TAGTGAGCAACCGGGCAT-3′	XbaI
F-CYP142A1	5′-**CATATG**ACTGAAGCTCCGGAC-3′	NdeI
R-CYP142A1	5′-**AAGCTT**TCAGCCCAGCGGCGGG-3′	HindIII
F-*E. coli* FNR	5′-**GCTAGC**ATGGCTGATTGGGTAACAG-3′	NheI
R-*E. coli* FNR	5′-**GAGCTC**TTACCAGTAATGCTCCGCT-3′	SacI
F-*E. coli* Flda	5′-**GCTAGC**ATGGCTATCACTGGCATCT-3′	NheI
R-*E. coli* Flda	5′-**GAGCTC**TCAGGCATTGAGAATTTCGT-3′	SacI

The restriction sites in the primers are depicted in bold. *E. coli, Escherichia coli*; F, forward primer; FNR, ferredoxin NADPH reductase; R, reverse primer.

CYP concentrations were quantified using the carbon monoxide difference spectrum assay according to Omura and Sato.[31]

Heterologous expression of FNR and Flda of *E. coli* was conducted as described by Neeli et al. and Hoover et al., respectively.[32,33] These redox partners were selected as surrogate electron transfers based on their previously reported ability to support catalytic activities of the selected Mtb CYPs.[20,24,34] UV-vis spectroscopic analysis of FNR and Flda showed spectra in line with those reported in previous studies displaying characteristic peaks at 370 nm and 450 nm for *E. coli* FNR and at 466 nm and 372 nm, with a distinct shoulder on the longer wavelength band at <495 nm, for the oxidized pure *E. coli* Flda (**Suppl. Fig. S2**).[35,36]

Analysis of Metabolism of D-Luciferin by Mtb CYPs

To determine whether the product D-luciferin is further metabolized by Mtb CYPs, which may obscure detection of D-luciferin formation from the pro-luciferin substrates, 0.5 µM D-luciferin was incubated with 0.5 µM Mtb CYP, 2.5 µM *E. coli* FNR, and 5 µM Flda in a final volume of 50 µL in 50 mM potassium phosphate buffer (pH 7.4) supplemented with 5 mM $MgCl_2$. The catalytically self-sufficient CYP130A1-BM3R fusion protein was also incubated at a concentration of 0.5 µM but in the absence of supplemental redox partners. As controls, incubations of 0.5 µM luciferin in buffer and 0.5 µM luciferin with only FNR and Flda were used. All incubations were performed in triplicate at 37 °C, except for CYP121A1, which was incubated at 30 °C, as in previous studies.[15,16] The reactions were performed in opaque white 96-well plates and were initiated by the addition of 5 µL 10× NADPH regenerating system, consisting of 5 mM NADPH, 100 mM glucose-6-phosphate, and 4 unit/mL glucose-6-phosphate dehydrogenase. After incubating for 1 h, 50 µL P450-Glo LDR was added, which terminates the CYP reaction and generates a luminescent signal that is proportional to the D-luciferin concentration.[37] Signals were allowed to stabilize for 20 min at room temperature, after which the luminescence was quantified as relative light units (RLUs) using a GloMax 96 Microplate Luminometer (Promega), operating without filters and with an integration time of 1 s per well. To quantify the metabolism of D-luciferin, the luminescence of incubations in the presence of Mtb CYPs was corrected for the background luminescence measured by performing control incubations in the absence of Mtb CYPs. Incubations with CYP125A1, which appeared to interfere with P450-Glo LDR reagent if not denatured (data not shown), were terminated by the addition of 5 µL 5 M trifluoroacetic acid and subsequently neutralized by 50 µL 1.5 M Tris buffer, pH 9.

In addition to the quantification of D-luciferin by the luminometric assay, D-luciferin and possible metabolites were analyzed by liquid chromatography–mass spectrometry (LC-MS). An Agilent 1200 rapid resolution LC system (Agilent, Santa Clara, CA, USA) was used connected to a time-of-flight (TOF) Agilent 6230 mass spectrometer and diode array detector. Analytes were separated using a Phenomenex Luna 5 µm C18 column (4.6 × 150 mm) protected by a Phenomenex security guard (5 µm, 4.0 × 3.0 mm) (Phenomenex, Torrance, CA, USA). A binary gradient running at 0.6 mL/min was used and was constructed using eluent A (0.1% formic acid, 98.9% H_2O, and 0.1 % acetonitrile) and eluent B (0.1% formic acid, 1% H_2O, and 98.9% acetonitrile). The gradient was programmed as follows: (1) from 0 to 5 min, isocratic at 1% B; (2) from 5 to 30 min, a linear increase from 1% B to 99% B; (3) from 30 to 35 min, isocratic at 99% B; (4) from 35 to 35.5 min, linear decrease from 99 to 1% B; and (5) from 35.5 to 45 min, isocratic at

1% B. The Agilent TOF 6230 mass spectrometer was equipped with an electrospray ionization source and was operating in positive ionization mode with a capillary voltage of 3500 V, 10 L/min nitrogen drying gas, and 50 psig nitrogen nebulizing gas at 350 °C. The data were analyzed using Agilent Masshunter Qualitative Analysis software, Version 5.0.

Metabolism of Luminogenic Substrates by Mtb CYPs

To evaluate the ability of the five Mtb CYPs to metabolize pro-luciferin substrates to D-luciferin, each Mtb CYP was incubated with 17 luminogenic substrates. Incubations were performed with 0.5 µM purified Mtb CYP, 2.5 µM *E. coli* FNR, and 5 µM Flda, in a final volume of 100 µL in 50 mM potassium phosphate buffer (pH 7.4) supplemented with 5 mM $MgCl_2$. Substrate concentrations used were 50 µM, except for Luciferin-IPA, Luciferin-1A2, and Luciferin-2B6, which were incubated at 25 µM because of their lower water solubility. The reactions were initiated by the addition of 10 µL 10× NADPH regenerating system, resulting in final concentrations of 0.5 mM NADPH, 10 mM glucose 6-phosphate, and 0.4 unit/mL glucose-6-phosphate dehydrogenase. All incubations were performed in triplicate in opaque white 96-well plates. The reactions were allowed to proceed for 1 h at 37 °C, with the exception of CYP121A1, which was incubated at 30 °C, as done previously.[15,16] Reactions were terminated by the addition of 100 µL P450-Glo LDR. For incubations with Luciferin-H EGE, Luciferin-ME EGE, and Luciferin-MultiCYP, the P450-Glo LDR was supplemented with 20 unit/mL porcine esterase to hydrolyze the ester group.[37] For incubations with Luciferin-1A2 and Luciferin-2B6, the P450-Glo LDR was supplemented with 4 mM D-cysteine to cyclize the cyano group to form D-luciferin.[37] After addition of the P450-Glo LDR, signals were allowed to stabilize for 20 min at room temperature, after which the luminescence was quantified using a GloMax 96 Microplate Luminometer, as described above. For each pro-luciferin substrate, control incubations were performed in the absence of Mtb CYPs to measure background luminescence. The background luminescence was subtracted from the luminescence measured in Mtb CYP–containing incubations to give the net RLU values.

The amounts of D-luciferin formed in the reactions were quantified using a standard curve of D-luciferin prepared in the reaction solutions. Triplicate samples at 2.0, 0.4, 0.08, 0.016, and 0.0 µM D-luciferin standards were used to construct a standard curve. The luminescence observed at 0 µM D-luciferin was subtracted from the luminescence measured in the presence of D-luciferin. Concentrations of D-luciferin were calculated by linear regression analysis using GraphPad Prism 8.02 for Windows (GraphPad Software, San Diego, CA, USA).

Assessment of Enzyme Kinetic Parameters

For enzyme–substrate pairs that showed significant luminescence, the enzyme kinetical parameters were determined by incubating with eight concentrations of luminogenic substrate in the presence and absence of 0.5 µM Mtb CYP. Concentrations were made by a twofold dilution series starting at either 250 or 500 µM. All incubations were performed in triplicate. Because the increase in luminescence was linear for at least 60 min (**Suppl. Fig. S3**), reactions were terminated after 60 min by the addition of 100 µL P450-Glo LDR. The mean background RLU values of incubations in the absence of Mtb CYPs were subtracted from the RLU values measured in the corresponding incubations in the presence of Mtb CYPs. The D-luciferin concentration was calculated from the net RLU values using a standard curve of D-luciferin, which was constructed as described above. Enzyme kinetic parameters K_m and V_{max} were determined by nonlinear regression according to the Michaelis–Menten equation using GraphPad Prism 8.02 for Windows (GraphPad Software).

Validation of the Bioluminescence Assay for CYP130A1-BM3R

The highest luminescence was produced after incubation of Luciferin-BE with CYP130A1-BM3R. To evaluate the robustness of the bioluminescence assay for HTS application, the Z'-factor and signal-to-background (S/B) ratio were determined according to Zhang et al.[38] As positive controls, 35 incubations were performed with 0.5 µM CYP130A1-BM3R and 100 µM Luciferin-BE, in a final volume of 50 µL in 50 mM potassium phosphate buffer (pH 7.4) supplemented with 5 mM $MgCl_2$. Reactions were initiated by the addition of 5 µL 10× NADPH regenerating system and allowed to proceed for 1 h at 37 °C. Reactions were terminated by the addition of 50 µL P450-Glo LDR, and luminescence was quantified after 20 min at room temperature, as described above. As a negative control, 35 incubations in the absence of CYP130A1-BM3R were also conducted. The S/B ratio was calculating by dividing the mean signal from the positive control by the mean signals from the negative control. The Z'-factor was calculated according to the following equation:[38]

$$Z' = 1 - \frac{3\left(\sigma_p + \sigma_n\right)}{\left|\mu_p - \mu_n\right|}$$

where μ_p and σ_p are the mean values and standard deviation, respectively, of the luminescence signals of the 35 incubations containing CYP130A1-BM3R; and μ_n and σ_n are those of the incubations without CYP130A1-BM3R.

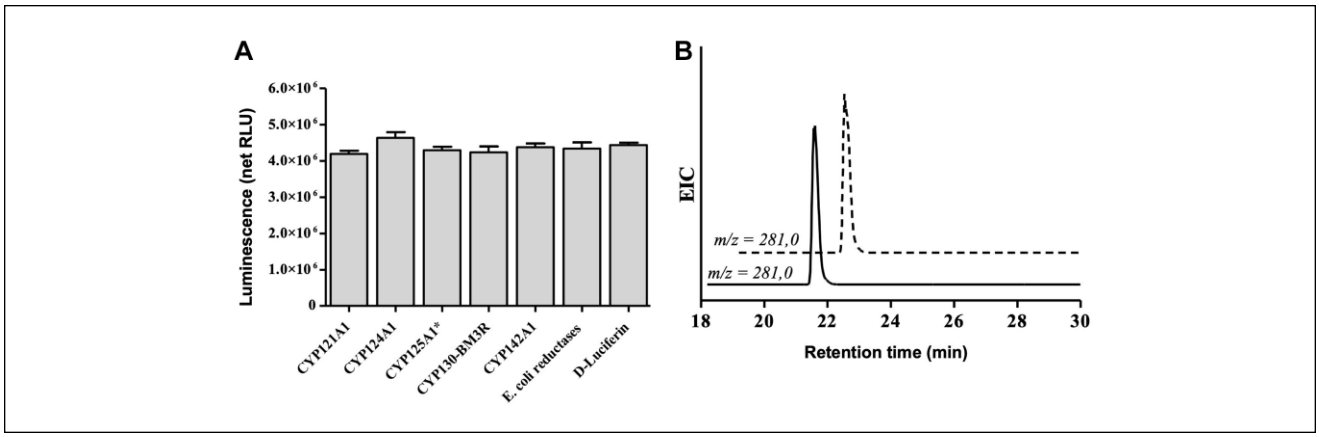

Figure 1. Evaluation of D-luciferin stability after incubation with *Mycobacterium tuberculosis* (Mtb) cytochrome P450 enzymes (CYPs). (**A**) D-luciferin luminescent signal after incubation of 0.5 µM D-luciferin with 0.5 µM Mtb CYPs. Bars represent means ± standard deviation (SD) of triplicate experiments. As negative controls, incubations of D-luciferin with only *Escherichia coli* FNR and Flda or D-luciferin in buffer were performed. CYP125A1*, incubations with CYP125A1 were terminated by acidification and neutralized before luminescence measurement, as described in the Materials and Methods section. (**B**) Representative extracted ion chromatograms of incubations with D-luciferin ($m/z = 281$) with CYP125A1: *solid line*, incubation terminated after 0 min of incubation; and *dotted line*, incubation terminated after 60 min of incubation.

Assessment of IC_{50} Values for a Selection of Azole Compounds

To determine the IC_{50} values for a selection of azole compounds, 0.5 µM CYP130A1-BM3R was pre-incubated for 10 min at 37 °C with 37 µM Luciferin-BE in the presence of varying concentrations of econazole, ketoconazole, and miconazole. Concentrations of these azole compounds were varied from 0.001 to 100 µM. The incubations were performed in triplicate in opaque white 96-well plates and in a final volume of 50 µL in 50 mM potassium phosphate buffer (pH 7.4) supplemented with 5 mM $MgCl_2$. The reactions were started by the addition of 5 µL 10× NADPH regenerating system and incubated for 1 h at 37 °C. Reactions were terminated by the addition of 50 µL of P450-Glo LDR, and luminescence was quantified as described above. Luminescence was corrected for the background luminescence measured in corresponding incubations performed in the absence of CYP130A1-BM3R. IC_{50} values were calculated using GraphPad Prism 8.02 for Windows (GraphPad Software) by nonlinear regression using the log(inhibitor concentration) versus a response equation with four-parameter logistic curve fitting.

Results and Discussion

Metabolism of D-Luciferin by Mtb CYPs

Since the use of pro-luciferin substrates relies on the formation of D-luciferin, whether D-luciferin can undergo secondary metabolism by the Mtb CYPs was studied first, because this would limit the application of D-luciferin-based screening assays. As shown in **Figure 1A**, the luminescent signal of D-luciferin was not significantly decreased after incubation for 1 h with CYP121A1, CYP124A1, CYP130A1-BM3R, CYP142A1, or the *E. coli* redox partners. Only after incubating with CYP125A1 was a strong decrease of luminescence observed (data not shown). LC-MS analysis of the incubation of D-luciferin with CYP125A1 did not, however, show a significant decrease of D-luciferin concentration and no product formation (**Fig. 1B**). Therefore, CYP125A1 seems to interfere with the luminescence detection by the P450-Glo LDR reagent. By terminating the CYP125A1 incubations with acid and neutralization, before adding P450-Glo LDR, the full luminescence of D-luciferin was obtained again (**Fig. 1A**). The mechanism by which active CYP125A1 interfered with the luminescence detection was not further investigated.

Metabolism of Pro-Luciferin Substrates by Mtb CYPs

Figure 2A–2E shows the production in net luminescence obtained after 60 min of incubation of the five Mtb CYPs with the 17 pro-luciferin substrates. The net luminescence production was calculated by subtracting the luminescence measured in control incubations without Mtb CYPs from the luminescence measured in incubations in the presence of Mtb CYPs. For the absolute luminescence measured in both conditions, see **Supplemental Figure S4**, which also shows the S/B ratio of the luminescence values.

As shown in **Figure 2D**, the highest increase in luminescence was observed in the incubations of CYP130A1-BM3R with Luciferin-BE as substrate. Using the standard curve of D-luciferin, the concentration of D-luciferin formed in the

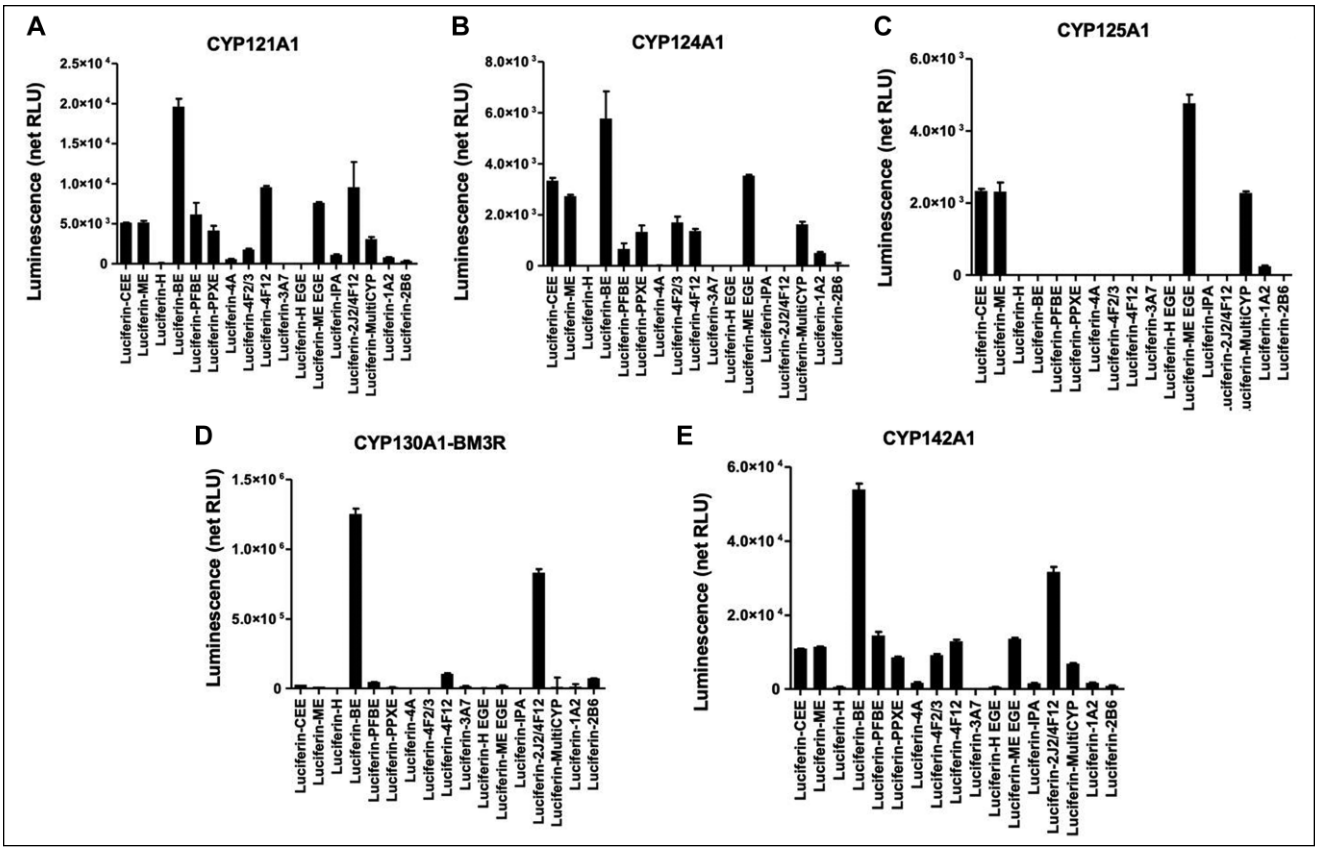

Figure 2. Luminescence produced after incubation of 17 luminogenic substrates for 60 min with five *Mycobacterium tuberculosis* (Mtb) cytochrome P450 enzymes (CYPs): (**A**) CYP121A1, (**B**) CYP124A1, (**C**) CYP125A1, (**D**) CYP130-BM3R, and (**E**) CYP142A1. Luminescence measured after incubations in the presence of 0.5 µM Mtb CYP and 100 µM luminogenic was corrected for background luminescence measured in control incubations in the absence of Mtb CYPs. All incubations were performed in triplicate; bars represent means ± standard deviation (SD). Absolute values of luminescence measured after incubations in the presence and absence of Mtb CYPs are presented in **Supplemental Figure S4**.

incubation of CYP130A1-BM3R with Luciferin-BE was determined to be 0.38 ± 0.01 µM (**Suppl. Fig. S5**). Incubation of Luciferin-BE with CYP130A1 reconstituted with *E. coli* FNR and Flda as redox partners resulted in a 4.5-fold lower amount D-luciferin formation (**Suppl. Fig. S6**). The higher activity of CYP130A1-BM3R can be explained by the more efficient electron transfer from the NADPH cofactor to the catalytic heme domain for the fusion protein, as was observed previously when using dextromethorphan as substrate.[25] For CYP130A1-BM3R also, a high activity was observed with Luciferin-2J2/4F12 as substrate, although with a 1.5-fold lower activity when compared to incubations with Luciferin-BE as substrate (**Fig. 2D**). Luciferin-4F12, Luciferin-2B6, and Luciferin-PFBE also showed significant increase of luminescence but at a 10-fold lower yield. Because Luciferin-BE appeared to be the best substrate for CYP130A1-BM3R, the enzyme kinetic parameters of the O-debenzylation reaction was determined by incubating with different substrate concentrations. As shown in **Figure 3**, when plotting the specific activity of D-luciferin formation against Luciferin-BE concentration, a hyperbolic curve was obtained for CYP130A1-BM3R. When fitted by nonlinear regression according to the Michaelis–Menten equation, a K_m of 37 ± 2.4 µM and k_{cat} of 40 ± 0.8 pmol D-luciferin/nmol CYP/min were obtained. When compared to the enzyme kinetic parameters of dextromethorphan N-demethylation, which was the first CYP130A1-BM3R-catalyzed reaction identified,[25] the O-debenzylation reaction of Luciferin-BE shows a 25-fold lower k_{cat} value and a 3.9-fold lower K_m value (**Table 2**). As a consequence, the intrinsic clearance k_{cat}/K_m for Luciferin-BE O-debenzylation appears 10-fold lower than that of dextromethorphan N-demethylation. Since the dextromethorphan N-demethylation requires a low-throughput high-performance liquid chromatography (HPLC)-based method, whereas the luminescence-based method allows parallel incubations in high-density microtiter plates, the latter method will be more suitable for HTS.

Compared to the luminescence observed after incubations with CYP130A1-BM3R and Luciferin-BE, only very low luminescence was observed after incubations with the other four Mtb CYPs (**Fig. 2**). For CYP121A1, the monooxygenase specific to the *Mycobacterium* genus, the highest net luminescence was also observed after incubations with Luciferin-BE (**Fig. 2A**). The S/B ratio of luminescence

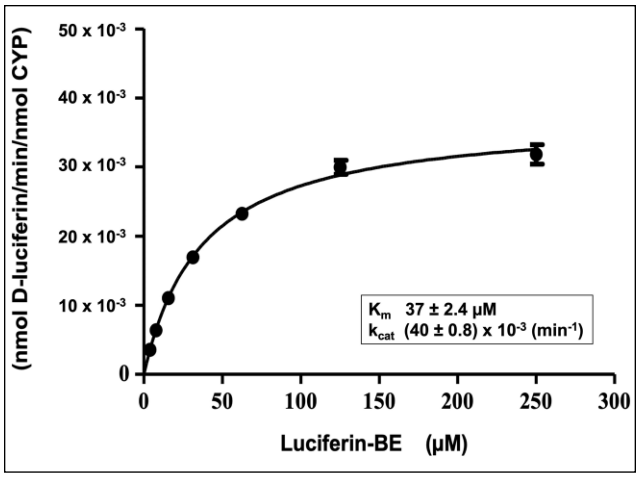

Figure 3. Enzyme kinetic analysis of D-luciferin formation in incubations of Luciferin-BE with CYP130A1-BM3R. The enzyme kinetic parameters were obtained by nonlinear regression according to the Michaelis–Menten equation. Points represent means ± standard deviation (SD) of triplicate experiments. Background D-luciferin formation was measured in incubations in the absence of CYP130A1-BM3R, and subtracted from D-luciferin formation in the presence of CYP130A1-BM3R.

was only 2.1, however (see **Suppl. Fig. S4**). CYP121A1 is known to specifically catalyze the C–C coupling of the aromatic rings of cYY, yielding mycocyclosin.[15,16] For this specialized Mtb CYP, no other substrates have been identified yet. Because of the low yields of luminescence and the low S/B ratios, the luminogenic substrates evaluated in the present study do not appear suitable for HTS for inhibitors of the Mtb CYP.

CYP124A1, CYP125A1, and CYP142A1 are known to catalyze 26-hydroxylation of the side chain of cholesterol and 4-cholestene-3-one.[39,40] When incubated with the luminogenic substrates, significant differences in selectivity were observed (**Fig. 2B**, **2C**, and **2E**). Luciferin-ME EGE was the only pro-luciferin substrate metabolized by these three cholesterol-metabolizing Mtb CYPs and showed the highest S/B values (7.3, 7.8, and 21 for CYP124A1, CYP125A1, and CYP142A1, respectively (see **Suppl. Fig. S4B**, **S4C**, and **S4E**). It was attempted to determine enzyme kinetic properties using this substrate. Because of the very low production of luminescence obtained at the lower substrate concentrations, however, not enough data points were obtained to describe hyperbolic curves for CYP124A1 and CYP125A1. Only for CYP142A1 could a hyperbolic curve be obtained (**Suppl. Fig. S7**), allowing assessment of its enzyme kinetic parameters (**Table 2**). When comparing the enzyme kinetic parameters obtained with those previously obtained for the hydroxylation of cholesterol and cholest-4-en-3-one, the K_m values were 23- to 35-fold higher with Luciferin-ME EGE as substrate, which is indicative of a significantly lower affinity. Furthermore, the catalytic efficiency k_{cat}/K_m of D-luciferin production appeared to be more than a millionfold lower when compared with those of cholesterol and cholest-4-en-one hydroxylation. This points to a predominantly nonproductive orientation of Luciferin-ME EGE in the active site of CYP142A1. Although the high sensitivity of luminescent detection of D-luciferin allowed the assessment of enzyme kinetic parameters, the magnitude of the luminescent signal is very low when compared to CYP130A1-BM3R.

Validation and Application of the Bioluminescence Assay for CYP130A1-BM3R

Since CYP130A1-BM3R showed the highest luminescence signal with Luciferin-BE as substrate, the robustness of this potential HTS assay was validated by determining the Z'-factor.[36] **Figure 4** shows the variability in luminescence of 35 incubations in the presence of CYP130A1-BM3R and of 35 incubations performed in the absence of CYP130A1-BM3R. Based on these data, a Z'-factor of 0.87 and an average S/B ratio of 65 was obtained. A Z'-factor higher than 0.5 is considered the threshold for robust HTS assays. Therefore, Luciferine-BE can be considered a valuable substrate for HTS for inhibitors of CYP130A1.

To demonstrate the applicability of this novel bioluminescence assay for the quantification of the inhibitory properties of ligands, the IC_{50} values of the three azole compounds were determined (**Fig. 5**). Econazole and miconazole appeared to be the most potent inhibitors of CYP130A1-BM3R with IC_{50} values equal to 0.05 ± 0.01 and 0.017 ± 0.003 μM, respectively. Ketoconazole showed

Table 2. Comparison of enzyme kinetic parameters of luminogenic substrates and previously reported substrates.

Mtb CYP	Substrate	K_m^{app} (μM)	k_{cat}^{app} (min^{-1})	k_{cat}/K_m (μM^{-1} min^{-1})	Reference
CYP130-BM3R	Dextromethorphan	143 ± 11	1.6 ± 0.1	11.2×10^{-3}	[24]
	Luciferin-BE	37 ± 2.4	$(40 \pm 0.8) \times 10^{-3}$	1.1×10^{-3}	This study
CYP142A1	Cholesterol	7.7 ± 2	16.7 ± 1.3	2.2	[40]
	Cholest-4-en-3-one	11.8 ± 1.5	84 ± 5	7.1	[40]
	Luciferin-ME-EGE	270 ± 22	$(61 \pm 5.8) \times 10^{-6}$	0.2×10^{-6}	This study

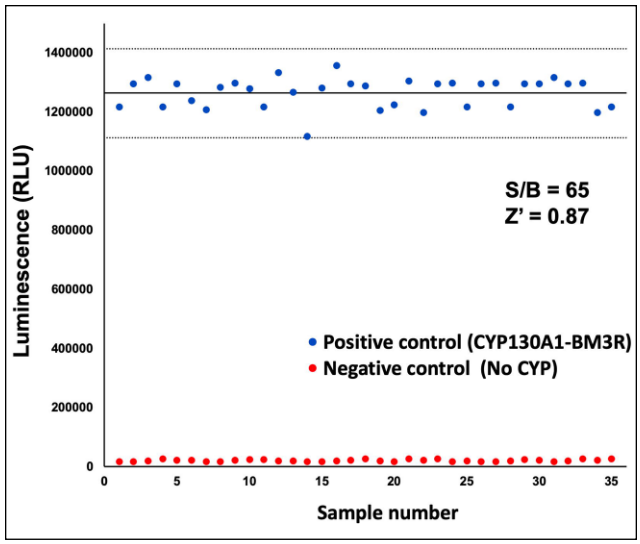

Figure 4. Assessment of Z'-factor for the high-throughput assay for CYP130A1-BM3R using Luciferin-BE as substrate. The assay was performed in 96-well microplate format. Each well contained 100 µM Luciferin, 0.5 µM CYP130A1-BM3R, and NADPH regenerating system (NRS) in a final volume of 50 µL in 50 mM phosphate buffer. After 60 min at 37 °C, reactions were terminated by addition of 50 µM P450-Glo Luciferin Detection Reagent (P450-Glo LDR), and incubated for an additional 20 min at room temperature before measuring luminescence. Red dots represent incubations in the absence of CYP130A1-BM3R, which were used as negative controls. The dashed lines represent ±3 standard deviations from the mean signal (solid line).

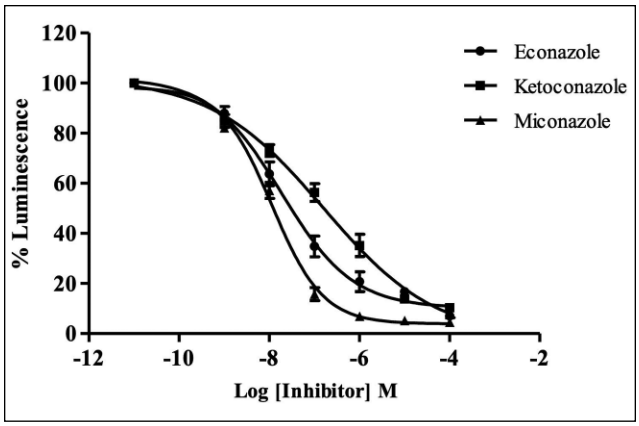

Figure 5. Concentration-dependent inhibition of CYP130A1-BM3R activity by azole compounds. Data are expressed as percentage of luminescence relative to luminescence of incubations in the absence of inhibitor. IC_{50} values calculated were as follows: econazole, 0.05 ± 0.01 µM; miconazole, 0.017 ± 0.003 µM; and ketoconazole, 0.1 ± 0.02 µM. Samples were analyzed as described under the Materials and Methods section (mean ± standard deviation, $n = 3$).

the lowest inhibitory potency with an IC_{50} value of 0.10 ± 0.02 µM. These IC_{50} values obtained are in accordance with the values previously reported using an HPLC-based method with dextromethorphan as substrate (**Table 3**).[25] Since the HPLC-based method requires 20 min analysis time per sample, however, whereas the luminescence-based method allows parallel measurement in high-density microplates, the novel assay will be more suitable for HTS.

Previous studies have used UV-vis spectroscopy to identify potent inhibitors of CYP130A1. By measuring the spectral shift caused by addition of 100 µM concentration of ligand to 0.8 µM CYP130A1, 20,000 compounds could be screened in 384-well plates.[42] Subsequent quantification of apparent dissociation constants (K_d) of positive hits by spectral titration, however, required titration of compounds to 1 mL of 2.5 µM of CYP130A1. In the novel bioluminescent assay, the enzyme concentration and incubation volume were fivefold (0.5 µM vs. 2.5 µM) and 20-fold (50 µL vs. 1 mL) lower, respectively, therefore requiring significantly less protein.[16] As shown in **Table 3**, the K_d values of the azole compounds obtained by spectral titration studies are 39- to 480-fold higher than the IC_{50} values obtained by enzyme inhibition experiments. Therefore, IC_{50} values are most likely more predictive for the inhibitory potency of compounds than K_d values obtained by spectral binding.

In conclusion, a novel and sensitive bioluminescent method has been established that is applicable for HTS for inhibitors of CYP130A1. Further structural optimization of luminogenic substrates is required for CYP121A1, CYP124A1, CYP125A1, and CYP142A1, however, since

Table 3. Comparison of IC_{50} and K_d values for a test set of inhibitors of CYP130A1-BM3R-catalyzed reactions.

Inhibitor	IC_{50} (this study), Luciferin-BE	IC_{50} (24), dextromethorphan	K_d values, dextromethorphan	Ratio K_d/IC_{50}, dextromethorphan
Econazole	0.05 ± 0.01	0.017 ± 0.007	1.93 ± 0.03	39
Ketoconazole	0.1 ± 0.02	0.13 ± 0.02	48 ± 1.5	480
Miconazole	0.017 ± 0.003	0.023 ± 0.006	1.70 ± 0.21	100

IC_{50} is expressed in µM.
Each data point represents a mean of triplicates ± standard deviation (SD).

the luminescent yield and S/B values with the tested substrates are considered too low to be used for HTS.

Abbreviations

CYP, Cytochrome P450; cYY, dicyclotyrosine; Flda, flavodoxin; FNR, ferredoxin NADPH reductase; HTS, high-throughput screening; LDR, luciferin detection reagent; Mtb, *Mycobacterium tuberculosis*; RLU, relative light units; TB, tuberculosis.

Declaration of Conflicting Interests

The authors declared no potential conflicts of interest with respect to the research, authorship, and/or publication of this article.

Funding

The authors disclosed receipt of the following financial support for the research, authorship, and/or publication of this article: This project was funded by The Netherlands Organization for Scientific Research (grant no. 022.005.031 to S. Ortega Ugalde).

References

1. Danielson, P. B. The Cytochrome P450 Superfamily: Biochemistry, Evolution and Drug Metabolism in Humans. *Curr. Drug Metab*. **2002**, *3*, 561–597.
2. Guengerich, F. Cytochrome P450s and Other Enzymes in Drug Metabolism and Toxicity. *APPS J*. **2006**, *8*, E101–E111.
3. Nelson, D. R. Cytochrome P450 Diversity in the Tree of Life. *Biochim. Biophys. Acta Proteins Proteom*. **2018**, *1866*, 141–154.
4. Kelly, S. L.; Kelly, D. E. Microbial Cytochromes P450: Biodiversity and Biotechnology. Where Do Cytochromes P450 Come from, What Do They Do and What Can They Do for Us? *Philos. Trans. R. Soc. B Biol. Sci*. **2013**, *368*, 20120476–20120476.
5. Lepesheva, G. I.; Waterman, M. R. Sterol 14α-Demethylase Cytochrome P450 (CYP51), a P450 in All Biological Kingdoms. *Biochim. Biophys. Acta*. **2007**, *1770*, 467–477.
6. Podust, L. M.; Stojan, J.; Poulos, T. L.; et al. Substrate Recognition Sites in 14-Alpha-Sterol-Demethylase from Comparative Analysis of Amino Acid Sequences and X-Ray Structure of *Mycobacterium tuberculosis* CYP51. *J. Inorg. Biochem*. **2001**, *87*, 227–235.
7. Podust, L. M.; Yermalitskaya, L. V.; Lepesheva, G. I.; et al. Estriol Bound and Ligand-Free Structures of Sterol 14α-Demethylase. *Structure*. **2004**, *12*, 1937–1945.
8. Chen, C. K.; Leung, S. S. F.; Guilbert, C.; et al. Structural Characterization of CYP51 from *Trypanosoma cruzi* and *Trypanosoma brucei* Bound to the Antifungal Drugs Posaconazole and Fluconazole. *PLoS Negl. Trop. Dis*. **2010**, *4*, e651.
9. Lepesheva, G. I.; Hargrove, T. Y.; Kleshchenko, Y.; et al. CYP51: A Major Drug Target in the Cytochrome P450 Superfamily. *Lipids*. **2008**, *43*, 1117–1125.
10. Ortiz De Montellano, P. R. Potential Drug Targets in the *Mycobacterium tuberculosis* Cytochrome P450 System. *J. Inorg Biochem*. **2018**, *180*, 235–245.
11. Ahmad, Z.; Sharma, S.; Khuller, G. K. In Vitro and Ex Vivo Antimycobacterial Potential of Azole Drugs against *Mycobacterium tuberculosis* H37Rv. *FEMS Microbiol. Lett*. **2005**, *251*, 19–22.
12. Ahmad, Z.; Sharma, S.; Khuller, G. K. The Potential of Azole Antifungals against Latent/Persistent Tuberculosis. *FEMS Microbiol. Lett*. **2006**, *258*, 200–203.
13. Ahmad, Z.; Sharma, S.; Khuller, G. K.; et al. Antimycobacterial Activity of Econazole against Multidrug-Resistant Strains of *Mycobacterium tuberculosis*. *Int. J. Antimicrob. Agents*. **2006**, *28*, 543–544.
14. McLean, K. J.; Cheesman, M. R.; Rivers, S. L.; et al. Expression, Purification and Spectroscopic Characterization of the Cytochrome P450 CYP121 from *Mycobacterium tuberculosis*. *J. Inorg. Biochem*. **2002**, *91*, 527–541.
15. Belin, P.; Le Du, M. H.; Fielding, A.; et al. Identification and Structural Basis of the Reaction Catalyzed by CYP121, an Essential Cytochrome P450 in *Mycobacterium tuberculosis*. *Proc. Natl. Acad. Sci. U.S.A*. **2009**, *106*, 7426–7431.
16. Fonvielle, M.; Le Du, M. H.; Lequin, O.; et al. Substrate and Reaction Specificity of *Mycobacterium tuberculosis* Cytochrome P450 CYP121: Insights from Biochemical Studies and Crystal Structures. *J. Biol. Chem*. **2013**, *288*, 17347–17359.
17. Taban, I. M.; Elshihawy, H. E. A. E.; Torun, B.; et al. Novel Aryl Substituted Pyrazoles as Small Molecule Inhibitors of Cytochrome P450 CYP121A1: Synthesis and Antimycobacterial Evaluation. *J. Med. Chem*. **2017**, *60*, 10257–10267.
18. Kishk, S. M.; McLean, K. J.; Sood, S.; et al. Synthesis and Biological Evaluation of Novel cYY Analogues Targeting *Mycobacterium tuberculosis* CYP121A1. *Bioorg. Med. Chem*. **2019**, *27*, 1546–1561.
19. McLean, K. J.; Lafite, P.; Levy, C.; et al. The Structure of *Mycobacterium tuberculosis* CYP125: Molecular Basis for Cholesterol Binding in a P450 Needed for Host Infection. *J. Biol. Chem*. **2009**, *84*, 35524–35533.
20. Driscoll, M. D.; McLean, K. J.; Levy, C.; et al. Structural and Biochemical Characterization of *Mycobacterium tuberculosis* CYP142: Evidence for Multiple Cholesterol 27-Hydroxylase Activities in a Human Pathogen. *J. Biol. Chem*. **2010**, *285*, 38270–38282.
21. Driscoll, M. D.; McLean, K. J.; Cheesman, M. R.; et al. Expression and Characterization of *Mycobacterium tuberculosis* CYP144: Common Themes and Lessons Learned in the *M. tuberculosis* P450 Enzyme Family. *Biochim. Biophys. Acta*. **2011**, *1814*, 76–87.
22. Ouellet, H.; Podust, L. M.; Ortiz de Montellano, P. R. *Mycobacterium tuberculosis* CYP130: Crystal Structure, Biophysical Characterization, and Interactions with Antifungal Azole Drugs. *J. Biol. Chem*. **2008**, *283*, 5069–5080.
23. Podust, L. M.; Ouellet, H.; von Kries, J. P.; et al. Interaction of *Mycobacterium tuberculosis* CYP130 with Heterocyclic Arylamines. *J. Biol. Chem*. **2009**, *284*, 25211–25219.
24. Johnston, J. B.; Kells, P. M.; Podust, L. M.; et al. Biochemical and Structural Characterization of CYP124: A Methyl-Branched Lipid Alpha-Hydroxylase from *Mycobacterium tuberculosis*. *Proc. Natl. Acad. Sci. U.S.A*. **2009**, *106*, 20687–20692.

25. Ortega Ugalde, S.; Luirink, R. A.; Geerke, D. P.; et al. Engineering a Self-Sufficient *Mycobacterium tuberculosis* CYP130 by Gene Fusion with the Reductase-Domain of CYP102A1 from *Bacillus megaterium*. *J. Inorg. Biochem*. **2018**, *180*, 47–53.
26. Fan, F.; Wood, K. Bioluminescent Assays for High-Throughput Screening. *Assay Drug Dev. Technol*. **2007**, *5*, 127–136.
27. Cali, J. J.; Ma, D.; Sobol, M.; et al. Luminogenic Cytochrome P450 Assays. *Expert Opin. Drug Metab. Toxicol*. **2006**, *2*, 629–645.
28. Cali, J. J.; Niles, A.; Valley, M. P.; et al. Bioluminescent Assays for ADMET. *Expert Opin. Drug Metab. Toxicol*. **2008**, *4*, 103–120.
29. Cali, J. J.; Ma, D.; Wood, M. G.; et al. Bioluminescent Assays for ADME Evaluation: Dialing in CYP Selectivity with Luminogenic Substrates. *Expert Opin. Drug Metab. Toxicol*. **2012**, *8*, 1115–1130.
30. Ortega Ugalde, S.; de Koning, C. P.; Wallraven, K.; et al. Linking Cytochrome P450 Enzymes from *Mycobacterium tuberculosis* to Their Cognate Ferredoxin Partners. *Appl. Microbiol. Biotechnol*. **2018**, *102*, 9231–9242.
31. Omura, T.; Sato, R. The Carbon Monoxide-Binding Pigment of Liver Microsomes. *J. Biol. Chem*. **1964**, *239*, 2370–2378.
32. Neeli, R.; Sabri, M.; McLean, K. J.; et al. Trp(359) Regulates Flavin Thermodynamics and Coenzyme Selectivity in *Mycobacterium tuberculosis* FprA. *Biochem. J*. **2008**, *411*, 563–570.
33. Hoover, D. M.; Ludwig, M. L. A Flavodoxin That Is Required for Enzyme Activation: The Structure of Oxidized Flavodoxin from *Escherichia coli* at 1.8 A Resolution. *Protein Sci*. **1997**, *6*, 2525–2537.
34. Ouellet, H.; Guan, S.; Johnston, J. B. *Mycobacterium tuberculosis* CYP125A1, a Steroid C27 Monooxygenase That Detoxifies Intracellularly Generated Cholest-4-en-3-one. *Mol. Microbiol*. **2010**, *77*, 730–742.
35. Jenkins, C. M.; Waterman, M. R. Flavodoxin and NADPH-Flavodoxin Reductase from *Escherichia coli* Support Bovine Cytochrome P450c17 Hydroxylase Activities. *Biochemistry* **1994**, *269*, 27401–27408.
36. McIver, L.; Leadbeater, C.; Campopiano, R. L.; et al. Characterisation of Flavodoxin $NADP^+$ Oxidoreductase and Flavodoxin; Key Components of Electron Transfer in *Escherichia coli*. *Eur. J. Biochem*. **1998**, *257*, 577–585.
37. Promega. Technical Bulletin: P450-GloTM Assays. https://www.promega.com/-/media/files/resources/protocols/technical-bulletins/101/p450-glo-assays-protocol.pdf (accessed May 13, 2019).
38. Zhang, J. H.; Chung, T. D.; Oldenburg, K. R. A Simple Statistical Parameter for Use in Evaluation and Validation of High Throughput Screening Assays. *J. Biomol. Screen*. **1999**, *4*, 67–73.
39. Johnston, J. B.; Ouellet, H.; Ortiz de Montellano, P. R. Functional Redundancy of Steroid C26-Monooxygenase Activity in *Mycobacterium tuberculosis* Revealed by Biochemical and Genetic Analyses. *J. Biol. Chem*. **2010**, *285*, 36352–36360.
40. Ouellet, H.; Guan, S.; Johnston, J. B.; et al. *Mycobacterium tuberculosis* CYP125A1, a Steroid C27 Monooxygenase That Detoxifies Intracellularly Generated Cholest-4-en-3-one. *Mol. Microbiol*. **2010**, *77*, 730–742.